

Confidence-calibrated covariate shift correction for few-shot classification in Vision-Language Models

Behraj Khan^{1,3} , Rizwan Qureshi² , Nouman Muhammad Durrani³ , Tahir Qasim Syed^{1*} 

¹School of Mathematics and Computer Science, Institute of Business Administration Karachi, Pakistan.

²Center for Research in Computer Vision, University of Central Florida, USA.

³National University of Computer and Emerging Sciences, Karachi, Pakistan.

{behrajkhan, tqsyed}@iba.edu.pk, tahirqsyed@gmail.com

Abstract

Since the establishment of vision-language foundation models as the new mainstay in low-shot vision classification tasks, the question of domain generalization arising from insufficient target data is assuming more importance. This scarcity challenge induces sampling bias and amplifies model sensitivity to variations and shifts in data distributions. While fine-tuning on multiple domains could mitigate such domain generalization issues, it is resource-intensive and demands diverse data sources. In this work, we systematically analyze two critical challenges: (1) covariate shift between the pre-training distribution and the underspecified target distribution, and (2) confidence misalignment, where predictions on novel data are overconfident. To address both challenges simultaneously, we introduce *Confidence-Calibrated Covariate Shift Correction (CalShift)*—a unified approach that combines a Fisher information penalty to mitigate covariate shift and a Confidence Misalignment Penalty (CMP) to reduce overconfidence in misclassified examples. Experimental evaluations across various vision and covariate shift benchmarks demonstrate that CalShift significantly improves model calibration, achieving up to a 5.82% reduction in Expected Calibration Error (ECE). Furthermore, CalShift enhances robustness, improving accuracy by 3.5% on challenging datasets impacted by covariate shifts. Our results highlight CalShift as a promising strategy for building robust and reliable low-shot vision-language systems for real-world applications.

1. Introduction

Foundation models such as CLIP [45], Flamingo [3], and Align [2] form the cornerstone of contemporary vision-language understanding systems, especially for downstream

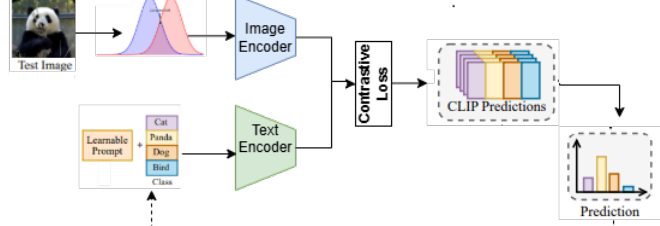
vision classification tasks in the emerging post-training paradigm. Their real-world deployment, while gaining ubiquity, has to contend with two significant challenges related to *domain generalization*, the ability to generalize to classification tasks close to but outside the pre-training distribution.

The first challenge is *covariate shift*, which occurs because the *feature distribution* between training and target data differs, $P(x)_{tr} \neq P(x)_{ts}$ while the conditional distribution remains unchanged $P(y|x)_{tr} = P(y|x)_{ts}$ [7, 27, 48, 50]. This phenomenon is inherent in domain generalization for foundation models because feature distributions differ by definition, and is garnering attention as a significant angle of the generalization regime [37, 60, 63].

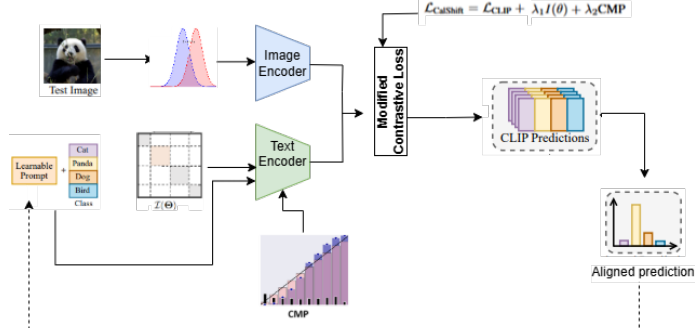
The second challenge, *confidence misalignment*, emerges when a model's predicted confidence (softmax) scores fail to accurately represent the true predictive likelihood because of mis-classifications [13, 15, 30]. By definition, confidence calibration is the alignment between predicted probabilities and the true correctness likelihood [39, 58]. This issue is particularly pronounced in few-shot post-training regimes, characterized by scarce labeled data, statistically unstable target distributions, and resulting unreliable predictions that are inadequately reflected in predictive confidence [26]. Confidence misalignment mirrors harmful forgetting in LLMs [23] when distribution shifts causes models uncertainty estimation to degrade. Similarly in our case, covariate shift can break the model confidence in VLMs, leading to overconfident errors.

Previous approaches such as [27] address the covariate shift problem caused by dataset fragmentation by regularizing the loss function with Fisher information penalty. [37] highlight calibration degradation of CLIP-based adaptation methods in presence of distribution shifts particularly in out-of-distribution (OOD) scenarios due to increased logit ranges. The authors propose a model-agnostic logit scaling approach to restore calibration while maintaining per-

* Corresponding author



(a) Misaligned predictions caused by covariate shift.



(b) Aligned predictions after integration of CMP and FIM $I(\theta)$.

Figure 1. Workflow of the proposed CalShift framework: The sub-figure (a) illustrates the confidence misalignment problem caused by covariate shift. The (bottom right) part of the sub-figure (a) show misaligned predictions. The subfigure (b) middle section represents the two components as recipe in method: Fisher Information Penalty ($I(\theta)$) for covariate shift correction and Confidence Misalignment Penalty (CMP) for calibration. Both FIM and CMP are integrated into the CLIP text encoder. The final loss, $\mathcal{L}_{\text{CalShift}} = \mathcal{L}_{\text{CLIP}} + \lambda_1 I(\theta) + \lambda_2 \text{CMP}$, combines the original CLIP loss with FIM and CMP to produce robust and aligned predictions, as shown in (bottom right) as output.

formance. [58] addresses the problem of miscalibration in vision-language models and the author propose data-based approach such as, dynamic outlier regularization (DOR). DOR mitigates the calibration problem by minimizing feature deviation for novel textual labels to balance calibration between new and base classes. [26] study the confidence calibration problem under covariate shift in low-shot setting for vision-language model. The authors resolve this problem using confidence alignment.

These approaches typically address either covariate shift or confidence misalignment independently. To fill this gap, we propose a unified framework, termed *Confidence-Calibrated Covariate Shift Correction (CalShift)*, which jointly addresses both challenges. Our method employs the popular Tikhonov regularization principle. It therefore integrates a Fisher information-based [31] penalty to mitigate covariate shift and a confidence misalignment penalty (CMP) to recalibrate confidence scores within the contrastive loss formulation of CLIP. CMP penalizes overconfident incorrect predictions by shifting log-likelihood to the true class. In doing so, CalShift provides a robust mechanism for achieving reliable and well-calibrated predictions in low-shot vision classification scenarios. The working mechanism of

our framework is shown in Figure 1.

Furthermore, our method CalShift aligns with growing interest in training-free adaptation, where a models adapts to new or unseen task without having access to any additional data at training time. Our methods allows VLMs to adapt to new target distribution in a training-free manner, making it highly effective in real-world applications where access to more training data is costly or infeasible.

Contributions

In this work, we bridge two distinct yet related areas of research by unifying penalties previously studied independently for covariate shift and confidence misalignment.

1. We introduce a loss component that suppresses CLIP’s confidence on misclassifications by moderating the flow of posterior likelihood towards any posterior peak higher than that of the true class.
2. We use knowledge about incorrect predictions existing as labels, which is inherently invariant to transformations such as data augmentation or batch/layer-normalization.
3. We discover that correcting for covariate shift in relaxed conditions of $P(x|y)$ not necessarily staying constant,

still helps improves calibration in real-world settings.

4. We offer improvements in the predictive envelope of a post-trained model along the axes of confidence calibration, trustworthiness and generalisation.

2. Related work

Vision-language foundation models. Foundation models open new horizons for machine learning tasks, particularly in supervised learning [24, 45]. Foundation models like CLIP can be easily adapted for downstream tasks. To further improve, downstream task classification, several efficient methods are available, including parameter-efficient prompt tuning (PEFT) [67], prompt tuning, vanilla fine-tuning [28], adapter tuning [65], and CLIP fine-tuning [14].

The CLIP foundation model [45], consist of an image encoder $f(x)$ and a text encoder $g(t)$. Both encoders are jointly trained using contrastive loss. The pre-trained CLIP provide support of few-shot learning which can then be used for downstream tasks like *prompt learning* using fixed or hand-crafted prompts. Context Optimization (CoOp) [67] introduced learnable task-specific prompts by replacing the manually designed prompts. CoOp provides two different prompt implementation i.e. *Unified context vectors* where prompts shared across classes and *Class-specific context vectors* provides individual prompts per class. But admittedly, CoOp struggles with generalization to unseen classes and distribution shift.

Distribution shift in foundation models. Distribution shifts present unique challenges for foundation models compared to traditional domain generalization or adaptation [20, 61]. In classical approaches, models are trained to learn invariant features under the assumption that these invariances hold at test time. In contrast, foundation models like CLIP [45], ALIGN [24], and Flamingo [3] are pre-trained on large-scale data and later adapted to downstream tasks. However, deploying these models in low-shot settings introduces challenges such as covariate shift (where the input distribution $P(x)$ differs between pretraining (source) and target data) and confidence misalignment (where the model becomes overconfident on shifted inputs) [26, 55, 57]. [23] highlighted how distribution shifts can induce confidence misalignment in VLMs and proposed “vaccine” approach, applying perturbation-aware confidence alignment during fine-tuning to mitigate harmful embedding shifts. We address confidence alignment in low-shot settings through calibration-aware regularization.

Confidence calibration in deep learning models. Extensive research focuses on confidence calibration methods to ensure model accuracy is aligned with its predicted confidence scores. These methods includes regularization based approaches, such as implicit regularization [47] [4], L_2 regularization [15] , and entropy regularization [44] to align the model predicted accuracy with confidence. Some

augmentation-based approaches, such as label-smoothing [36] and mix-up training methods [52, 64] are also explored for confidence calibration in deep learning models. [40] empirically investigated the calibration of deep learning models under distribution shift. A comprehensive survey [55], which addresses the recent development about calibration for deep learning models.

Confidence calibration in foundation models. [41] addresses the issue of under-confidence in pre-trained foundation models when these models are fine-tuned for downstream tasks in few-shot settings. Similarly, [37] highlights the miscalibration problem in CLIP-based adaptive approaches. Their proposed method empirically demonstrates that CLIP-based adaptive approaches, such as prompt learning, adapters, parameter-efficient fine-tuning (PEFT), and test-time adaptation, are prone to miscalibration in low-shot settings under distribution shifts. Furthermore, [53] investigates the prediction uncertainty of the foundation model CLIP for image classification tasks, focusing on variations in visual factors. Recent work [58] observed observed the post-hoc confidence miscalibration in fine-tuned VLMs and proposed Distance-Aware Calibration (DAC) to align calibration of VLMs.

In this work, we propose a regularization-based approach to ensure that the predictive probabilities of foundation models align with confidence scores in a prompt-learning setting under distribution shifts.

3. Method

Contrastive Language–Image Pretraining (CLIP) is a multimodal model developed by [45] that learns latent-space image-text association from large datasets and enables zero-shot transfer learning to diverse vision tasks. CLIP uses contrastive loss (\mathcal{L}_c for image-text alignment can be defined as:

$$\mathcal{L}_c = \frac{1}{2} (\mathcal{L}_{\text{txt}} + \mathcal{L}_{\text{img}}),$$

while, text loss is given as:

$$\mathcal{L}_{\text{txt}} = -\frac{1}{N} \sum_{i=1}^N \log \frac{\exp(\text{sim}(\mathbf{t}_i, \mathbf{i}_i)/\tau)}{\sum_{j=1}^N \exp(\text{sim}(\mathbf{t}_i, \mathbf{i}_j)/\tau)},$$

and image loss is denoted as:

$$\mathcal{L}_{\text{img}} = -\frac{1}{N} \sum_{i=1}^N \log \frac{\exp(\text{sim}(\mathbf{i}_i, \mathbf{t}_i)/\tau)}{\sum_{j=1}^N \exp(\text{sim}(\mathbf{i}_i, \mathbf{t}_j)/\tau)}.$$

Covariate shift: In low-shot learning regimes, availability of limited data may be insufficient to bring the post-training distribution simulate the pre-training distribution, which leads to poor generalization. Similarly, when data are distributed across batches or folds, each subset represents

an extremely low-data setting, where distribution shift emerges due to insufficient sample representation *between* any two subsets of post-training data. The information loss due to covariate shift caused by such fragmented data partitions [35, 51] can be effectively measured by Fisher information [1, 8, 27], very similar to in low-shot learning scenarios in classical transfer learning.

Fisher information in covariate shift. Fisher Information has been shown to an equivalent of relative entropy without iterative computation, and accesses the curvature of the parameter surface to measure even small perturbation [31, 34]. Fisher information measures the sensitivity of model to change in data distribution makes it ideal solution to diagnose and mitigate shift in covariates in VLMs. The Fisher information measure can be defined as:

$$I(\theta) = -\mathbb{E} \left[\frac{\partial^2 \log P(X; \theta)}{\partial \theta^2} \right] \quad (1)$$

where $I(\theta)$ is Fisher information which can be defined as the negative hessian of the log-likelihood function $-\mathbb{E} \left[\frac{\partial^2 \log P(X; \theta)}{\partial \theta^2} \right]$ [31, 34].

Recently, the FI matrix was used to compute and by consequence, help correct, divergence in data distributions under a batched-streaming setting [27]. We are possibly the first to borrow the idea into the VLM post-training regime.

Confidence misalignment: Foundation models such as CLIP are often overconfident in fine-tuned predictions when image-text pair does not reconcile, specifically in low-shot settings [26, 37, 41, 53]. The CLIP contrastive loss maximizes \mathcal{L}_c for correct image-text pair while minimizing it for incorrect pairs. Evidence is emerging of **neural collapse** in the final phase of training/fine-tuning/post-training[42]. It is noticed that intra-class examples close in or collapse towards the class mean. The rescaling by the softmax to 1 may further reduces numerical variability. The higher and narrower peak encourage over-confidence, regardless of the correctness of the classification, which results in $H(P(\mathbf{t}|\mathbf{i}; \theta)) \rightarrow 0$.

Fisher information and CMP. Fisher information addresses the distribution shift and uncertainty caused by covariate shift while CMP helps in reliability and calibration of model. Both challenges are closely linked: As covariate shift exacerbates confidence misalignment by creating distributional discrepancies, whereas overconfident predictions can obscure the underlying uncertainty caused by distribution shifts [27, 37].

To overcome the overconfidence problem, the confidence misalignment penalty (CMP) is introduced by [26], which draws likelihood away from a text-image-pair mismatch. This likelihood is moved into the matching class

from each mismatched class pair in proportion to the mismatched likelihood. That excess likelihood is:

$$\text{CMP} = \frac{P(x, y)}{\sum_{y' \neq y, P(x, y') > P(x, y)} P(x, y')}, \quad (2)$$

where $P(x, y)$ is the softmax probability for the correct pair (\mathbf{i}, \mathbf{t}) , while $P(x, y')$ is the softmax probability for incorrect pairs $(\mathbf{i}, \mathbf{t}')$, where $t \neq t'$.

CalShift which combines Fisher information and CMP into a single cohesive approach and jointly regularize the CLIP contrastive loss, This holistic approach provides a non-post-hoc way for confidence calibration under covariate shift of VLMs in few-shot learning regimes. CalShift controls misalignment, thereby enhancing VLM reliability under distribution shifts and reducing harmful overconfidence in safety-critical applications.

Proposition 3.1 *The Fisher information $I(\theta)$ improves generalization by controlling the curvature of the loss landscape and CMP improves calibration by penalizing overconfidence and redistributing log-likelihood to the true class.*

The Fisher information $I(\theta)$ in eq 1 measures the curvature of log-likelihood function with respect to model parameters θ . A high $I(\theta)$ indicates sharp curvature which results in poor generalization. To mitigate this effect, we introduce Fisher information regularization by adding $\lambda_1 I(\theta)$ into the loss function:

$$\mathcal{L}_{\text{CalShift}} = \mathcal{L}_c + \lambda_1 I(\theta).$$

From PAC-Bayes perspective [19, 59], $I(\theta)$ tightens the generalization bound by controlling the complexity of hypothesis class. The PAC-Bayes bound for a model with parameters θ is:

$$\mathcal{E}_{\text{gen}}(\theta) \leq \mathcal{E}_{\text{emp}}(\theta) + \frac{I(\theta) + \log(1/\delta)}{2n}$$

where, $\mathcal{E}_{\text{gen}}(\theta)$ is generalization error and can be defined as:

$$\mathcal{E}_{\text{gen}}(\theta) = \mathbb{E}_{(x, y) \sim P_{\text{test}}} [\ell(f_{\theta}(x), y)],$$

while $\mathcal{E}_{\text{emp}}(\theta)$ is empirical error and is given by:

$$\mathcal{E}_{\text{emp}}(\theta) = \frac{1}{n} \sum_{i=1}^n \ell(f_{\theta}(x_i), y_i),$$

θ is confidence parameter and n is number of training samples. Minimization of $I(\theta)$, reduce $\mathcal{E}_{\text{gen}}(\theta)$, ensures model robustness to distribution shift.

The second term, CMP given in eq 2 penalizes overconfidence by redistributing log-likelihood to the true class, it ensures that does not assign excessively high probabilities

to incorrect classes. To mitigate overconfidence we integrate $\lambda_2 \text{CMP}$ into loss function:

$$\mathcal{L}_{\text{CalShift}} = \mathcal{L}_c + \lambda_2 \text{CMP}.$$

From a Bayesian perspective, CMP act as regularization that encourage the model to distribute probability mass more uniformly across plausible classes. This helps in model calibration by aligning the predicted probabilities with actual correctness likelihood.

From the Minimum Description Length (MDL) principle [16, 25, 66], the CMP reduces the complexity of learned hypothesis by controlling overconfident predictions. The MDL bound for a model with θ parameters can be defined as:

$$\mathcal{E}_{\text{gen}}(\theta) \leq \mathcal{E}_{\text{emp}}(\theta) + \frac{\mathcal{C}(\theta) + \log(1/\delta)}{2n}.$$

Where $\mathcal{C}(\theta)$ is hypothesis complexity. By minimizing CMP, model effectively reduces the hypothesis complexity, provides a more compact representation that generalizes better. It helps the model to form robust decision boundaries.

$I(\theta)$ regularization ensures that representations remain robust under domain shifts and CMP ensures that the model does not become overconfident, improving calibration. Since neither penalty degrades the other's effect, CalShift optimally balances robustness and calibration. Thus, minimizing the loss function given in eq 3, guarantees a pareto-optimal balance between robustness to covariate shift and also preserving the confidence calibration.

$$\mathcal{L}_{\text{CalShift}}(x, y; \theta) = \mathcal{L}_c + \lambda_1 I(\theta) + \lambda_2 \text{CMP} \quad (3)$$

More detail on the theoretical background about $I(\theta)$ and CMP can be found in Appendix A.

4. Experiments and Results

4.1. Experiments

Datasets. To check the effectiveness of CalShift, we used 19 vision dataset including natural distribution datasets, domain adaptation datasets and vision classification datasets used for evaluation by low-shot prompt learning methods. These datasets are: Caltech101 [12], Imagenet [9], EuroSAT [18], StanfordCars [29], FGVCAircraft [33], OxfordPets [43], SUN397 [62], Food101 [5], Flowers102 [38], DTD [6], UCF101 [49], PACS [32], VLCS [11], Office-Home [54] and five domain adaptation datasets such as Imagent-1k and its variants like ImageNet A (Art) [22], ImageNet-V2 (V2) [46], ImageNet R (Real) [21] and ImageNet S (Sketch) [56].

Baselines. We consider CLIP and prompt learning method CoOp[67] without any penalty integration as baseline in

comparison to our method.

Evaluation metrics. We used accuracy (Acc) as evaluation metric for robustness of CalShift under covariate shift and vision datasets used by prompt learning approaches, while Expected Calibration Error (ECE) [15] is used with same number of datasets for evaluating the calibration performance of CalShift.

Implementation details. To check the robustness and calibration performance of CalShift, we conduct extensive experiments on various datasets. We used pre-trained CLIP [45] with ViT-B/16 [10] as backbone in prompt learning method. In covariate shift experiment we used CLIP with ViT-B/16 and ResNet-50 backbone [17] for the last four variants of ImageNet. For first four datasets we follow the same protocol of [32], where model is trained on another domain and evaluated on another test domain.

The experimental detail, datasets, and evaluation metrics used in the paper can be found in appendix 4.1. here,

we discuss the robustness and confidence calibration results of our method CalShift.

4.2. Results

Calshift generalization performance across shots. Table 1 upper part shows the generalization performance of CalShift across incremental few-shot settings. It is shown in Table 1 that the integration of FIM with CoOp consistently outperforms CLIP and vanilla CoOp across all shot settings. CalShift achieves a maximum accuracy improvement of 6.8% over CoOp in the zero-shot setting and 7.2% in the 1-shot setting. CalShift shows a 5.9% average accuracy improvement over CoOp, demonstrating that CalShift regularization effectively mitigates overfitting in data-scarce regimes.

The $\Delta\%$ decrease monotonically from 7.2% (1-shot) to 5.1% (16-shot) settings, which shows the effectiveness of CalShift in extremely low-shot data regime. This provides empirical strength to FIM's role in stabilizing gradient updates when labeled examples are scarce. Furthermore, in a zero-shot setting with no training data, integrating FIM with CoOp surpasses CLIP, demonstrating FIM's superior ability to retain knowledge compared to CoOp alone. This suggests that FIM acts as a prior-preserving regularizer, preventing CLIP from catastrophic forgetting in zero-shot scenarios.

Calshift calibration performance across shots. CalShift's calibration performance results are shown in the lower half of Table 1. Integrating CMP with CoOp consistently outperforms vanilla CoOp across all few-shot settings, achieving up to a 12.5% improvement in the 4-shot setting and 10.2% in the 16-shot scenario. In the zero-shot scenario,

Table 1. Few-shot accuracy (%) on ImageNet with CalShift. The Δ row in upper half of the table shows improvement (\uparrow) or degradation (\downarrow) in accuracy over baseline. The bottom half of the table shows Expected Calibration Error (ECE %) on ImageNet with and without CMP penalty. In ECE scenario lower is better. Δ shows percentage improvement (\downarrow) or degradation (\uparrow).

		Number of shots							
		Method	0	1	2	4	8	16	Avg.
ACC	CLIP	72.4	68.1	70.3	73.6	75.9	77.2	72.9	
	CoOp	79.5	75.2	77.8	80.1	82.4	83.7	79.8	
	CoOp + FIM	84.9	80.6	82.1	84.4	86.7	88.0	84.5	
	Δ %	6.8 \uparrow	7.2 \uparrow	5.5 \uparrow	5.4 \uparrow	5.2 \uparrow	5.1 \uparrow	5.9 \uparrow	
ECE	CLIP	1.51	2.89	2.67	2.12	1.98	1.75	2.15	
	CoOp	3.36	3.12	2.94	2.88	2.64	2.45	2.90	
	CoOp + CMP	3.06	2.84	2.71	2.52	2.38	2.20	2.62	
	Δ %	8.93 \downarrow	8.97 \downarrow	7.82 \downarrow	12.50 \downarrow	9.85 \downarrow	10.20 \downarrow	9.66 \downarrow	

Table 2. The upper half shows CalShift accuracy results on vision datasets with and without FIM penalty. The Δ row shows the percentage increase (\uparrow) or decrease (\downarrow) in accuracy. The lower half shows CalShift ECE results on vision datasets with and without CMP penalty. The Δ row shows the percentage increase (\uparrow) decrease (\downarrow) in calibration

	Method	UCF101	Food101	Caltech101	OxfordPets	Flowers102	ImageNet	StanfordCars	FGVCAircraft	SUN397	DTD	EuroSAT	Avg.
ECE	CLIP	69.9	90.1	96.8	91.2	72.1	72.4	63.3	27.2	69.4	53.3	56.5	69.3
	CoOp	78.6	97.0	98.6	98.2	79.2	79.5	59.2	25.2	63.0	52.5	53.8	71.2
	CoOp + FIM	84.3	98.7	98.8	98.9	85.5	84.9	54.3	27.2	66.8	55.1	49.2	73.5
	Δ %	7.3 \uparrow	1.7 \uparrow	0.2 \uparrow	0.7 \uparrow	8.0 \uparrow	6.8 \uparrow	8.2 \downarrow	7.9 \uparrow	6.0 \uparrow	4.9 \uparrow	8.6 \downarrow	3.2 \uparrow
ACC	CLIP	3.24	1.57	6.49	2.25	3.11	1.51	3.74	3.03	1.59	4.53	9.12	3.52
	CoOp	3.08	3.35	3.24	3.06	2.96	3.36	3.38	3.24	3.02	3.06	3.08	3.16
	CoOp + CMP	2.94	3.02	3.08	2.84	3.16	3.06	3.16	3.08	2.96	2.92	3.06	2.98
	Δ %	4.55 \downarrow	9.85 \downarrow	4.94 \downarrow	7.19 \downarrow	6.76 \uparrow	8.93 \downarrow	6.51 \downarrow	4.94 \downarrow	1.99 \downarrow	4.57 \downarrow	0.65 \downarrow	5.70 \downarrow

CLIP’s calibration performance surpasses CoOp, indicating that prompt tuning can degrade CLIP’s calibration. Integrating CMP into CoOp mitigates this issue, improving calibration by 8.93% in the zero-shot setting.

Integrating CMP into CoOp improves $\Delta\%$ by a maximum of 8.97% in the 1-shot setting and 10.2% in the 16-shot setting, demonstrating CMP’s ability to better leverage additional data for confidence calibration. Table 1 demonstrates that integrating CMP into CoOp outperforms both vanilla CoOp and CLIP beyond the 4-shot setting, suggesting that CMP enhances calibration adaptation. This suggests that CMP tackles CoOp’s two key issues by penalizing overconfident logits: (1) overfitting in few-shot scenarios and (2) gradient misalignment. CMP addresses overfitting by enforcing decision boundary constraints, preventing overconfidence on limited data. Meanwhile, it mitigates misalignment by aligning logit gradients with true class margins, reducing bias in probability estimates.

Table 1 shows that FIM integration significantly enhances generalization, particularly in low-shot regimes, while CMP integration improves calibration in these settings. These results establish CalShift as a versatile

regularizer, ensuring robust and trustworthy adaptation in vision-language models.

CalShift robustness in vision tasks. The results in Table 2 demonstrates the effectiveness of FIM penalty integration into CoOP as compared to baselines. The Δ row in Table 2 shows improvement across most datasets. The notable improvement in accuracy include Imagenet (6.8%), Flowers102 (8.0%), and UCF101 (7.3%), indicates significant improvement, from action recognition to fine-grained classification. In scene and texture-based datasets CalShift shows robustness performance improvement with SUN397 (6.0%) and DTD (4.9%). For Food101 (1.7%), Caltech101 (0.2%), and OxfordPets (0.7%) improvement in accuracy. CalShift improves in accuracy by 3.2% on average across all datasets.

CalShift calibration in vision tasks. The CMP penalty-based calibration performance results across eleven vision datasets are shown in Table 2. In Table 2, it is shown that CMP integration improves in calibration for most datasets with an average of 5.70% reduction in calibration.

Table 3. The upper part shows CalShift accuracy results on covariate shift vision datasets with and without FIM penalty. The Δ row shows the percentage increase/decrease in accuracy. \uparrow shows improvement in accuracy while the \downarrow shows decrease in performance. The lower part shows CalShift ECE results on covariate shift vision datasets with and without CMP penalty. The Δ row shows the percentage increase/decrease in calibration. \downarrow shows improvement in calibration while \uparrow shows calibration performance decrease.

	Method	PACS	Office-Home	VLCS	DomainNet	ImageNet-V2	ImageNet-S	ImageNet-A	ImageNet-R
ACC	CLIP	96.1	80.4	81.4	54.1	60.8	46.2	47.8	73.9
	CoOp	96.5	82.1	82.5	58.8	64.2	47.9	49.7	75.2
	CoOp+FIM	98.0	85.6	86.0	60.0	65.5	48.8	50.5	76.8
	Δ %	1.5 \uparrow	3.5 \uparrow	3.5 \uparrow	1.2 \uparrow	1.3 \uparrow	0.9 \uparrow	0.8 \uparrow	1.6 \uparrow
ECE	CLIP	2.18	2.77	2.89	3.69	2.44	4.88	8.34	3.51
	CoOp	2.02	2.92	3.01	3.29	4.19	8.40	15.34	3.12
	CoOp+CMP	1.91	2.75	2.84	3.15	4.05	8.18	15.00	2.95
	Δ %	5.45 \downarrow	5.82 \downarrow	5.64 \downarrow	4.26 \downarrow	3.34 \downarrow	2.62 \downarrow	2.21 \downarrow	5.45 \downarrow

Smaller values are better in the calibration case. Penalty-based CoOp shows 9.85% calibration improvement at maximum on Food101, mageNet (8.93%), and OxfordPets (7.19%), which demonstrates CMP alignment in model calibration in these settings. On other datasets also it shows better performance such as, UCF101 (4.55%), Caltech101 (4.94%), StanfordCars (6.51%), and FGVC Aircraft (4.94%).

In comparison to CLIP, CoOP is surpassed by CLIP but when penalty is added then CoOp shows better calibration. Integration of penalty improves calibration across almost all datasets except Flowers102, where calibration is slightly worsen. The results provides an empirical evidence that penalty integration is reliable technique for reducing overconfidence and improving model reliability in low-shot learning.

Comparing penalty-bases CoOp to CLIP, penalty-based enhancement provides significant improvement across almost all datasets except StanfordCars and EuroSAT. CalShift shows UCF101 (14.4%), Flowers102 (13.4%), and ImageNet (12.5%) improvement at maximum in comparison to CLIP.

The integration of FIM penalty generally shows improvement in accuracy in low-shot vision tasks in particular when combined with prompt learning methods.

CalShift robustness in covariate shift. Table 3 shows the robustness performance of CalShift on eight domain generalization datasets under covariate shift. The Δ of Table 3 shows the penalty-based CoOp outperform CoOp across all datasets, showing significant improvement in robustness to covariate shift. CalShift shows maximum robustness performance in Office-Home (3.5%) and VLCS (3.5%) demonstrating FIM integration enhances adaptation across domain adaptation tasks. For all other datasets such

as, DomainNet (1.2%), ImageNet-V2 (1.3%), ImageNet-S (0.9%), ImageNet-A (0.8%), and ImageNet-R (1.6%), CalShift shows slight better improvement, suggesting better robustness in challenging real-world distribution shift.

While comparing penalty-based CoOp to CLIP, we observe consistent improvement in accuracy across all domain generalization datasets like, VLCS (4.6%) , Office-Home (5.2%) and PACS (1.9%). CalShift demonstrates better robustness on more challenging variants of ImageNet such as, ImageNet-V2 (1.3%) , ImageNet-S (2.6%), ImageNet-A (2.7%), and ImageNet-R (2.9%).

The FIM penalty indicates consistent performance improvement across covariate shift datasets, reinforcing the FIM penalty role in domain generalization and robustness to covariate shift datasets.

CalShift calibration in covariate shift. Table 3 presents, calibration performance of penalty integration into CoOp for covariate shift vision datasets. It is demonstrated, that CalShift improves in calibration across all datasets with an average of 2.21% at minimum and 5.82% at maximum. CalShift shows calibration improvement on Office-Home (5.82%), PACS (5.45%), VLCS (5.64%), ImageNet-R (5.45%) DomainNet (4.26%) and ImageNet-V2 (3.34%), while smaller but consistent improvements are seen in ImageNet-S (2.62%) and ImageNet-A (2.21%), which indicates the CMP effectiveness in confidence alignment on these datasets.

CLIP shows better calibration as compared to CoOP by reporting lower ECE such as, PACS (2.18 vs. 2.02), VLCS (2.89 vs. 3.01), and ImageNet-R (3.51 vs. 3.12). However, when penalty is integrated into CoOp, the calibration reduces significantly making it more comparable to CLIP.

Ablation of loss components. We evaluate the per-

formance of our proposed architecture by conducting ablation studies to understand the relative contribution of each component, Fisher information and CMP. We ablate the model by keeping the Fisher information $I(\theta)$ hyperparameter $\lambda_1 = 0$ in Equation 3 and then perform the experiment. Similarly, we set the CMP hyperparameter $\lambda_2 = 0$ and conduct another experiment. The results are reported in Table 4 and Table 5, respectively.

Effect of Fisher Information. Table 4 evaluates the isolated contributions of CMP and FIM across 11 vision datasets. The upper part of the table presents CalShift’s generalization performance with $\lambda_1 = 0$ and $\lambda_2 = 0.4$. CalShift demonstrates generalization efficacy, achieving a maximum improvement of 3.3% on Flowers102, 1.9% on SUN397, and 2.6% on ImageNet. However, it shows only marginal accuracy gains on OxfordPets and Caltech101, suggesting that CMP’s effect diminishes when CLIP features are already sufficient.

The lower part of Table 4 presents CalShift’s accuracy across 11 vision datasets with $\lambda_1 = 0.4$ (FIM-only) and $\lambda_2 = 0$ (no-CMP). CalShift achieves a maximum accuracy improvement of 5.2% on FGVC Aircraft, 7.4% on EuroSAT, and 4.9% on Flowers102.

Effect of misalignment penalty. Table 5 shows isolated calibration effect of CalShift across 11 vision datasets. The upper section of the Table shows ECE results with $\lambda_1 = 0$ (no FIM) and $\lambda_2 = 0.4$ (CMP only). CalShift improves in ECE by 2.7% on Flowers102 suggesting Calshift align well with balanced label distributions. However, limited gains on CLIP-compatible datasets 1.96% on OxfordPets and 1.3% on EuroSAT.

The lower section of the Table 5 with $\lambda_1 = 0.4$ (FIM-only) and $\lambda_2 = 0$ (no-CMP). It is shown in Table that CalShift consistently enhances calibration, reducing average ECE by 1.90%. Notable improvements occur on fine-grained datasets like StanfordCars -1.78% and class-balanced benchmarks such as Flowers102: -4.05%, demonstrating FIM ability to stabilize confidence estimates by penalizing overparameterized gradients.

Effect of λ_1 tuning on CalShift performance. Table 6 given in appendix B shows accuracy performance on four datasets, including Flowers102, Food101, UCF101, and DTD, for different values of λ_1 within the range (0.0 to 1.0), while λ_2 remains fixed at 0. $\lambda_1 = 0$ serves as the baseline with no Fisher penalty. The results in the table indicate that CalShift achieves the highest performance at $\lambda_1 = 0.4$, with accuracies of 98.8% on Food101, 84.3% on UCF101, and 55.1% on DTD, whereas performance declines for all other values.

Effect of λ_2 tuning on CalShift performance. In appendix Table 7 shows the calibration results of CalShift when tuning λ_2 within range (0.0 to 1.0) while λ_1 value fixed to 0. It is show in Table that with $\lambda_2 = 0.4$ CalShift achieve better calibration results across four dataset. The Calshift calibration performance drops on other values of λ_2 , while value 0.4 balance between over-regularization and under-regularization.

Our method is effective in confidence alignment as it shows better ECE consistently on almost all datasets. These results favors CalShift calibration reliability under covariate shift, making it more trustworthy in real-world applications.

5. Conclusions

This work introduces **CalShift**, a unified framework designed to address two critical challenges in low-shot vision tasks using foundation models: *covariate shift* and *confidence misalignment*. By integrating *Fisher Information* and *Confidence Misalignment Penalty (CMP)*, CalShift significantly enhances both *robustness* and *calibration* across various vision and domain generalization benchmarks. Experimental results show that CalShift (Confidence-Calibrated Covariate Shift Correction), built within the CalShift framework, consistently outperforms existing methods in terms of accuracy and calibration. Specifically, it achieves up to a **3.5% gain in accuracy** and reduces **Expected Calibration Error (ECE) by up to 5.82%** on challenging covariate shift datasets. These findings underscore CalShift’s promise as a reliable solution for real-world deployment, especially in low-shot scenarios where distribution shifts and overconfidence are prevalent. Future directions include extending the framework to *continual learning*, *online adaptation*, and test-time adaptation, where the model must remain calibrated under evolving distributions.

CalShift is well-suited for scenarios like test-time adaptation where model adapts to unseen (from a ststistics point of view, shifted) data distribution at inference time. The integration of Fisher information and CMP provides robust adaptation to distribution shift without need of additional training data. This makes it an effective solution particularly in those real-world applications where test-time condition vary from those during training.

The issue of confidence misalignment is not just a technical challenge but a critical challenge in AI alignment, leading to unsafe and unreliable decisions in safety-critical systems such as medical diagnosis and autonomous vehicles. Our method CalShift ensures that model predictions is aligned with human expectation.

Acknowledgments

The lead author experimented at NCBC-Video Surveillance Lab at FAST-NUCES Karachi, led by Prof. Muhammad Atif Tahir.

References

- [1] Adaptive filtering and hypothesis testing: Application to cancerous cells detection. *Pattern recognition letters*, 31(14):2214–2224, 2010. 4
- [2] Jameel Abdul Samad, Mohammad Hanan Gani, Noor Hussein, Muhammad Uzair Khattak, Muhammad Muzammal Naseer, Fahad Shahbaz Khan, and Salman H Khan. Align your prompts: Test-time prompting with distribution alignment for zero-shot generalization. *Advances in Neural Information Processing Systems*, 36, 2024. 1
- [3] Jean-Baptiste Alayrac, Jeff Donahue, Pauline Luc, Antoine Miech, Iain Barr, Yana Hasson, Karel Lenc, Arthur Mensch, Katherine Millican, Malcolm Reynolds, et al. Flamingo: a visual language model for few-shot learning. *Advances in neural information processing systems*, 35:23716–23736, 2022. 1, 3
- [4] Bahram K Baloch, Sateesh Kumar, Sanjay Haresh, Abeerah Rehman, and Tahir Syed. Focused anchors loss: Cost-sensitive learning of discriminative features for imbalanced classification. In *Asian Conference on Machine Learning*, pages 822–835. PMLR, 2019. 3
- [5] Lukas Bossard, Matthieu Guillaumin, and Luc Van Gool. Food-101-mining discriminative components with random forests. In *Computer vision–ECCV 2014: 13th European conference, Zurich, Switzerland, September 6–12, 2014, proceedings, part VI 13*, pages 446–461. Springer, 2014. 5
- [6] Mircea Cimpoi, Subhransu Maji, Iasonas Kokkinos, Sammy Mohamed, and Andrea Vedaldi. Describing textures in the wild. In *Proceedings of the IEEE conference on computer vision and pattern recognition*, pages 3606–3613, 2014. 5
- [7] Corinna Cortes and Mehryar Mohri. Domain adaptation and sample bias correction theory and algorithm for regression. *Theoretical Computer Science*, 519:103–126, 2014. 1
- [8] Thomas A Courtade. Monotonicity of entropy and fisher information: a quick proof via maximal correlation. *arXiv preprint arXiv:1610.04174*, 2016. 4
- [9] Jia Deng, Wei Dong, Richard Socher, Li-Jia Li, Kai Li, and Li Fei-Fei. Imagenet: A large-scale hierarchical image database. In *2009 IEEE conference on computer vision and pattern recognition*, pages 248–255. Ieee, 2009. 5
- [10] Alexey Dosovitskiy. An image is worth 16x16 words: Transformers for image recognition at scale. *arXiv preprint arXiv:2010.11929*, 2020. 5
- [11] Yuming Fang, Weisi Lin, Zhenzhong Chen, Chia-Ming Tsai, and Chia-Wen Lin. A video saliency detection model in compressed domain. *IEEE transactions on circuits and systems for video technology*, 24(1):27–38, 2013. 5
- [12] Li Fei-Fei, Rob Fergus, and Pietro Perona. Learning generative visual models from few training examples: An incremental bayesian approach tested on 101 object categories. *Computer Vision and Pattern Recognition Workshop*, 2004. 5
- [13] Yarin Gal and Zoubin Ghahramani. Dropout as a bayesian approximation: Representing model uncertainty in deep learning. In *international conference on machine learning*, pages 1050–1059. PMLR, 2016. 1
- [14] Peng Gao, Shijie Geng, Renrui Zhang, Teli Ma, Rongyao Fang, Yongfeng Zhang, Hongsheng Li, and Yu Qiao. Clip-adapter: Better vision-language models with feature adapters. *International Journal of Computer Vision*, 132(2):581–595, 2024. 3
- [15] Chuan Guo, Geoff Pleiss, Yu Sun, and Kilian Q Weinberger. On calibration of modern neural networks. In *International conference on machine learning*, pages 1321–1330. PMLR, 2017. 1, 3, 5
- [16] Mark H Hansen and Bin Yu. Model selection and the principle of minimum description length. *Journal of the american statistical association*, 96(454):746–774, 2001. 5
- [17] Kaiming He, Xiangyu Zhang, Shaoqing Ren, and Jian Sun. Deep residual learning for image recognition. In *Proceedings of the IEEE conference on computer vision and pattern recognition*, pages 770–778, 2016. 5
- [18] Patrick Helber, Benjamin Bischke, Andreas Dengel, and Damian Borth. Eurosat: A novel dataset and deep learning benchmark for land use and land cover classification. *IEEE Journal of Selected Topics in Applied Earth Observations and Remote Sensing*, 12(7):2217–2226, 2019. 5
- [19] Fredrik Hellström, Giuseppe Durisi, Benjamin Guedj, Maxim Raginsky, et al. Generalization bounds: Perspectives from information theory and pac-bayes. *Foundations and Trends® in Machine Learning*, 18(1):1–223, 2025. 4
- [20] Dan Hendrycks and Thomas Dietterich. Benchmarking neural network robustness to common corruptions and perturbations. *Proceedings of the International Conference on Learning Representations*, 2019. 3
- [21] Dan Hendrycks, Steven Basart, Norman Mu, Saurav Kadvath, Frank Wang, Evan Dorundo, Rahul Desai, Tyler Zhu, Samyak Parajuli, Mike Guo, et al. The many faces of robustness: A critical analysis of out-of-distribution generalization. In *Proceedings of the IEEE/CVF international conference on computer vision*, pages 8340–8349, 2021. 5
- [22] Dan Hendrycks, Kevin Zhao, Steven Basart, Jacob Steinhardt, and Dawn Song. Natural adversarial examples. In *Proceedings of the IEEE/CVF conference on computer vision and pattern recognition*, pages 15262–15271, 2021. 5
- [23] Tiansheng Huang, Siyao Hu, and Ling Liu. Vaccine: Perturbation-aware alignment for large language models against harmful fine-tuning attack. *arXiv preprint arXiv:2402.01109*, 2024. 1, 3
- [24] Chao Jia, Yinfei Yang, Ye Xia, Yi-Ting Chen, Zarana Parekh, Hieu Pham, Quoc Le, Yun-Hsuan Sung, Zhen Li, and Tom Duerig. Scaling up visual and vision-language representation learning with noisy text supervision. In *International conference on machine learning*, pages 4904–4916. PMLR, 2021. 3
- [25] Adam Tauman Kalai and Santosh S Vempala. Calibrated language models must hallucinate. In *Proceedings of the 56th Annual ACM Symposium on Theory of Computing*, pages 160–171, 2024. 5
- [26] Behraj Khan and Tahir Syed. Technical report on label-informed logit redistribution for better domain generalization in low-shot classification with foundation models. *arXiv preprint arXiv:2501.17595*, 2025. 1, 2, 3, 4

[27] Behraj Khan, Behroz Mirza, and Tahir Syed. Causal covariate shift correction using fisher information penalty. In *The Second Tiny Papers Track at ICLR 2024*. 1, 4

[28] Muhammad Uzair Khattak, Hanoona Rasheed, Muhammad Maaz, Salman Khan, and Fahad Shahbaz Khan. Maple: Multi-modal prompt learning. In *Proceedings of the IEEE/CVF Conference on Computer Vision and Pattern Recognition*, pages 19113–19122, 2023. 3

[29] Jonathan Krause, Michael Stark, Jia Deng, and Li Fei-Fei. 3d object representations for fine-grained categorization. In *Proceedings of the IEEE international conference on computer vision workshops*, pages 554–561, 2013. 5

[30] Ananya Kumar, Percy S Liang, and Tengyu Ma. Verified uncertainty calibration. *Advances in Neural Information Processing Systems*, 32, 2019. 1

[31] Erich L Lehmann and George Casella. *Theory of point estimation*. Springer Science & Business Media, 2006. 2, 4

[32] Da Li, Yongxin Yang, Yi-Zhe Song, and Timothy M Hospedales. Deeper, broader and artier domain generalization. In *Proceedings of the IEEE international conference on computer vision*, pages 5542–5550, 2017. 5

[33] Subhransu Maji, Esa Rahtu, Juhu Kannala, Matthew Blaschko, and Andrea Vedaldi. Fine-grained visual classification of aircraft. *arXiv preprint arXiv:1306.5151*, 2013. 5

[34] Ryan Martin. Lecture notes on advanced statistical theory. *Supplement to the lectures for Stat*, 511, 2016. 4

[35] Jose García Moreno-Torres, José A Sáez, and Francisco Herrera. Study on the impact of partition-induced dataset shift on k -fold cross-validation. *IEEE transactions on neural networks and learning systems*, 23(8):1304–1312, 2012. 4

[36] Rafael Müller, Simon Kornblith, and Geoffrey E Hinton. When does label smoothing help? *Advances in neural information processing systems*, 32, 2019. 3

[37] Balamurali Murugesan, Julio Silva-Rodríguez, Ismail Ben Ayed, and Jose Dolz. Robust calibration of large vision-language adapters. In *European Conference on Computer Vision*, pages 147–165. Springer, 2025. 1, 3, 4

[38] Maria-Elena Nilsback and Andrew Zisserman. Automated flower classification over a large number of classes. In *2008 Sixth Indian conference on computer vision, graphics & image processing*, pages 722–729. IEEE, 2008. 5

[39] Changdae Oh, Hyeji Hwang, Hee-young Lee, YongTaek Lim, Geunyoung Jung, Jiyoung Jung, Hosik Choi, and Kyungwoo Song. Blackvip: Black-box visual prompting for robust transfer learning. In *Proceedings of the IEEE/CVF Conference on Computer Vision and Pattern Recognition*, pages 24224–24235, 2023. 1

[40] Yaniv Ovadia, Emily Fertig, Jie Ren, Zachary Nado, David Sculley, Sebastian Nowozin, Joshua Dillon, Balaji Lakshminarayanan, and Jasper Snoek. Can you trust your model’s uncertainty? evaluating predictive uncertainty under dataset shift. *Advances in neural information processing systems*, 32, 2019. 3

[41] Deep Shankar Pandey, Spandan Pyakurel, and Qi Yu. Be confident in what you know: Bayesian parameter efficient fine-tuning of vision foundation models. In *The Thirty-eighth Annual Conference on Neural Information Processing Systems*, 2024. 3, 4

[42] Vardan Papyan, XY Han, and David L Donoho. Prevalence of neural collapse during the terminal phase of deep learning training. *Proceedings of the National Academy of Sciences*, 117(40):24652–24663, 2020. 4

[43] Omkar M Parkhi, Andrea Vedaldi, Andrew Zisserman, and CV Jawahar. Cats and dogs. In *2012 IEEE conference on computer vision and pattern recognition*, pages 3498–3505. IEEE, 2012. 5

[44] Gabriel Pereyra, George Tucker, Jan Chorowski, Łukasz Kaiser, and Geoffrey Hinton. Regularizing neural networks by penalizing confident output distributions. *arXiv preprint arXiv:1701.06548*, 2017. 3

[45] Alec Radford, Jong Wook Kim, Chris Hallacy, Aditya Ramesh, Gabriel Goh, Sandhini Agarwal, Girish Sastry, Amanda Askell, Pamela Mishkin, Jack Clark, et al. Learning transferable visual models from natural language supervision. In *International conference on machine learning*, pages 8748–8763. PMLR, 2021. 1, 3, 5

[46] Benjamin Recht, Rebecca Roelofs, Ludwig Schmidt, and Vaishaal Shankar. Do imagenet classifiers generalize to imagenet? In *International conference on machine learning*, pages 5389–5400. PMLR, 2019. 5

[47] T-YLPG Ross and GKHP Dollár. Focal loss for dense object detection. In *proceedings of the IEEE conference on computer vision and pattern recognition*, pages 2980–2988, 2017. 3

[48] Hidetoshi Shimodaira. Improving predictive inference under covariate shift by weighting the log-likelihood function. *Journal of statistical planning and inference*, 90(2):227–244, 2000. 1

[49] K Soomro. Ucf101: A dataset of 101 human actions classes from videos in the wild. *arXiv preprint arXiv:1212.0402*, 2012. 5

[50] Masashi Sugiyama and Klaus-Robert Müller. Input-dependent estimation of generalization error under covariate shift. 2005. 1

[51] Masashi Sugiyama, Matthias Krauledat, and Klaus-Robert Müller. Covariate shift adaptation by importance weighted cross validation. *Journal of Machine Learning Research*, 8(5), 2007. 4

[52] Sunil Thulasidasan, Gopinath Chennupati, Jeff A Bilmes, Tanmoy Bhattacharya, and Sarah Michalak. On mixup training: Improved calibration and predictive uncertainty for deep neural networks. *Advances in neural information processing systems*, 32, 2019. 3

[53] Weijie Tu, Weijian Deng, and Tom Gedeon. Toward a holistic evaluation of robustness in clip models. *arXiv preprint arXiv:2410.01534*, 2024. 3, 4

[54] Shivaram Venkataraman, Zongheng Yang, Davies Liu, Eric Liang, Hossein Falaki, Xiangrui Meng, Reynold Xin, Ali Ghodsi, Michael Franklin, Ion Stoica, et al. Sparkr: Scaling r programs with spark. In *Proceedings of the 2016 International Conference on Management of Data*, pages 1099–1104, 2016. 5

[55] Cheng Wang. Calibration in deep learning: A survey of the state-of-the-art. *arXiv preprint arXiv:2308.01222*, 2023. 3

[56] Haohan Wang, Songwei Ge, Zachary Lipton, and Eric P Xing. Learning robust global representations by penalizing local predictive power. *Advances in Neural Information Processing Systems*, 32, 2019. 5

[57] Shuoyuan Wang, Yixuan Li, and Hongxin Wei. Understanding and mitigating miscalibration in prompt tuning for vision-language models. *arXiv preprint arXiv:2410.02681*, 2024. 3

[58] Shuoyuan Wang, Jindong Wang, Guoqing Wang, Bob Zhang, Kaiyang Zhou, and Hongxin Wei. Open-vocabulary calibration for fine-tuned clip. In *Forty-first International Conference on Machine Learning*, 2024. 1, 2, 3

[59] Zifeng Wang, Shao-Lun Huang, Ercan E Kuruoglu, Jimeng Sun, Xi Chen, and Yefeng Zheng. Pac-bayes information bottleneck. *arXiv preprint arXiv:2109.14509*, 2021. 4

[60] Bingbing Wen, Chenjun Xu, HAN Bin, Robert Wolfe, Lucy Lu Wang, and Bill Howe. Mitigating overconfidence in large language models: A behavioral lens on confidence estimation and calibration. In *NeurIPS 2024 Workshop on Behavioral Machine Learning*. 1

[61] Mitchell Wortsman, Gabriel Ilharco, Jong Wook Kim, Mike Li, Simon Kornblith, Rebecca Roelofs, Raphael Gontijo Lopes, Hannaneh Hajishirzi, Ali Farhadi, Hongseok Namkoong, et al. Robust fine-tuning of zero-shot models. In *Proceedings of the IEEE/CVF conference on computer vision and pattern recognition*, pages 7959–7971, 2022. 3

[62] Jianxiong Xiao, James Hays, Krista A Ehinger, Aude Oliva, and Antonio Torralba. Sun database: Large-scale scene recognition from abbey to zoo. In *2010 IEEE computer society conference on computer vision and pattern recognition*, pages 3485–3492. IEEE, 2010. 5

[63] Zehao Xiao, Jiayi Shen, Mohammad Mahdi Derakhshani, Shengcui Liao, and Cees GM Snoek. Any-shift prompting for generalization over distributions. In *Proceedings of the IEEE/CVF Conference on Computer Vision and Pattern Recognition*, pages 13849–13860, 2024. 1

[64] Linjun Zhang, Zhun Deng, Kenji Kawaguchi, and James Zou. When and how mixup improves calibration. In *International Conference on Machine Learning*, pages 26135–26160. PMLR, 2022. 3

[65] Renrui Zhang, Rongyao Fang, Wei Zhang, Peng Gao, Kunchang Li, Jifeng Dai, Yu Qiao, and Hongsheng Li. Tip-adapter: Training-free clip-adapter for better vision-language modeling. *arXiv preprint arXiv:2111.03930*, 2021. 3

[66] Zirui Zhao, Wee Sun Lee, and David Hsu. Large language models as commonsense knowledge for large-scale task planning. *Advances in Neural Information Processing Systems*, 36, 2024. 5

[67] Kaiyang Zhou, Jingkang Yang, Chen Change Loy, and Ziwei Liu. Learning to prompt for vision-language models. *International Journal of Computer Vision*, 130(9):2337–2348, 2022. 3, 5

A. Theoretical Background

Proposition A.1 The Fisher information $I(\theta)$ is equal to the Kullback-Leibler (KL) divergence D_{KL} between the source distribution $p(X)$ and target distribution $q(X)$, providing a measure of covariate shift.

Proof A.1 Let $p(X; \theta)$ is probability density function parameterized by θ and $q(X)$ is underlying true distribution. The D_{KL} between $p(X; \theta)$ and $q(X)$ is given by:

$$D_{KL}(q(X) \parallel p(X; \theta)) = \mathbb{E}_{q(X)} [\log q(X) - \log p(X; \theta)].$$

By def. of Fisher information matrix (FIM):

$$I(\theta) = -\mathbb{E}_{p(X; \theta)} \left[\frac{\partial^2 \log P(X; \theta)}{\partial \theta^2} \right].$$

Under smoothing condition $onp(X; \theta)$, D_{KL} can be approximated using FIM.

$$D_{KL}(q(X) \parallel p(X; \theta)) \approx \frac{1}{2}(\theta_q - \theta)^T I(\theta)(\theta_q - \theta).$$

where, θ_q is optimal parameter which best fit $q(X)$. By taking second order Taylor expansion of $\log p(X; \theta)$ around θ_q :

$$\begin{aligned} \log p(X; \theta) &\approx \log p(X; \theta_q) + (\theta - \theta_q)^T \nabla_{\theta} \log p(X; \theta_q) \\ &\quad + \frac{1}{2}(\theta - \theta_q)^T H(\theta - \theta_q) \end{aligned}$$

where $H = \nabla_{\theta}^2 \log p(X; \theta)$ is the Hessian.

By taking expectation w.r.t to $q(X)$, the first term vanishes as Fisher information expectation is defined over second order derivative. The D_{KL} simplifies to:

$$D_{KL}(q(X) \parallel p(X; \theta)) \approx \frac{1}{2}(\theta_q - \theta)^T I(\theta)(\theta_q - \theta).$$

Thus, Fisher information provide a measure of divergence between $q(X)$ and $p(X; \theta)$, capturing covariate shift.

Proposition A.2 The Confidence Misalignment Penalty (CMP) provides the measure for degree of overconfidence in incorrect predictions and also ensures alignment between predicted and true confidence score. CMP ensures that it is always a valid confidence $0 \leq \text{CMP} \leq 1$, $\text{CMP} \approx 1$ when model is overconfidence, and $\text{CMP} \approx 0$ when the model is well-calibrated.

Proof A.2 Let CMP be defined as:

$$\text{CMP} = \frac{P(x, y')}{\sum_{y_j \neq y' : P(x, y_j) > P(x, y')} P(x, y_j)}$$

where, $P(x, y')$ is probability of predicted class y' . The denominator considers only y_j where $P(x, y_j) > P(x, y')$,

which means that CMP is small when all other classes have higher confidence than true class y' .

If the model is highly confident with incorrect prediction, then $P(x, y')$ is high, it can be expressed mathematically as:

$$\lim_{P(x, y') \rightarrow 1} \text{CMP} = 1$$

In case of well-calibration, the confidence mass is distributed across all other classes, reducing $P(x, y')$, ensuring $\text{CMP} \rightarrow 0$:

$$\lim_{P(x, y') \rightarrow 0} \text{CMP} = 0$$

Since all probabilities sum to 1, CMP is always within range $[0, 1]$, making it a valid calibration measure.

$$0 \leq \text{CMP} \leq 1$$

Thus, CMP acts as confidence misalignment penalty, discouraging overconfident yet incorrect predictions.

Proposition A.3 Integration of CMP and $I(\theta)$ into loss function ensures covariate shift correction and confidence calibration as well.

Proof A.3 The final modified CLIP loss given by:

$$\mathcal{L}_{\text{CalShift}}(x, y; \theta) = \mathcal{L}_c + \lambda_1 I(\theta) + \lambda_2 \text{CMP}$$

Where, As per theorem A.1, $I(\theta)$ addresses covariate shift, while proposition A.2 ensures confidence calibration.

In gradient update, $I(\theta)$ adjust the weight updates based on local curvature, prevents divergence due to covariate shift:

$$\Delta \theta \propto I(\theta)^{-1} \nabla \mathcal{L}(\theta)$$

where $I(\theta)^{-1}$ is scaling gradient to account local curvature while $\mathcal{L}(\theta)$ is the loss function.

CMP reduces the magnitude of updates to address the high confidence:

$$\nabla \text{CMP} \cdot \nabla \mathcal{L}(\theta) \approx 0 \quad \text{when confidence is high.}$$

If $\lambda_2 > 0$, then CMP ensure probability mass is distributed across classes rather than overly concentrating on incorrect prediction:

$$\lambda_2 > 0 \implies \sum_{y \neq y'} P(x, y)$$

This implies that when $\lambda_2 > 0$ then probability mass is distributed among classes. Tuning λ_1, λ_2 properly prevents overconfidence without penalising well-aligned distributions.

Thus, minimizing $\mathcal{L}_{\text{CalShift}}$ ensures well-calibrated robust prediction under covariate shift.

B. Ablation study

Table 4. The upper part of the table shows CalShift accuracy results while keeping Fisher Information penalty $I(\theta)$ ($\lambda_1 = 0$) and CMP penalty ($\lambda_2 = 0.4$). The Δ row shows the percentage increase (\uparrow) or decrease (\downarrow) in accuracy compared to CoOp. The lower part of the table CalShift accuracy results while keeping CMP penalty ($\lambda_2 = 0$) and FIM penalty $\lambda_1 = 0.4$. The Δ row shows the percentage increase (\uparrow) or decrease (\downarrow) in accuracy compared to CoOp.

Method	UCF101	Food101	Caltech101	OxfordPets	Flowers102	ImageNet	StanfordCars	FGVCAircraft	SUN397	DTD	EuroSAT	Avg.
CLIP	69.9	90.1	96.8	91.2	72.1	72.4	63.3	27.2	69.4	53.3	56.5	69.3
CoOp	78.6	97.0	98.6	98.2	79.2	79.5	59.2	25.2	63.0	52.5	53.8	71.2
CoOp + CMP ($\lambda_1 = 0$)	81.5	97.5	98.6	98.4	81.8	81.6	57.8	26.0	64.2	53.6	51.2	71.9
$\Delta \%$	3.7 \uparrow	0.5 \uparrow	0.0 \rightarrow	0.2 \uparrow	3.3 \uparrow	2.6 \uparrow	2.4 \downarrow	3.2 \uparrow	1.9 \uparrow	2.1 \uparrow	4.8 \downarrow	1.0 \uparrow
ACC												
CoOp	78.6	97.0	98.6	98.2	79.2	79.5	59.2	25.2	63.0	52.5	53.8	71.2
CoOp + FIM ($\lambda_2 = 0$)	82.3	97.9	98.5	98.7	83.1	82.9	57.2	26.5	65.8	54.5	49.8	72.6
$\Delta \%$	4.7 \uparrow	0.9 \uparrow	0.1 \downarrow	0.5 \uparrow	4.9 \uparrow	4.3 \uparrow	3.4 \downarrow	5.2 \uparrow	4.4 \uparrow	3.8 \uparrow	7.4 \downarrow	2.0 \uparrow

Table 5. The upper half of the table shows CalShift ECE results on vision datasets with and without FIM penalty $\lambda_1 = 0$ and CMP penalty ($\lambda_2 = 0.4$). The Δ row shows the percentage increase (\uparrow) or decrease (\downarrow) in calibration error. CalShift ECE results on vision datasets with and without CMP penalty ($\lambda_2 = 0$) and FIM penalty ($\lambda_1 = 0.4$). The Δ row shows the percentage increase (\uparrow) or decrease (\downarrow) in calibration error.

Method	UCF101	Food101	Caltech101	OxfordPets	Flowers102	ImageNet	StanfordCars	FGVCAircraft	SUN397	DTD	EuroSAT	Avg.
CoOp	3.08	3.35	3.24	3.06	2.96	3.36	3.38	3.24	3.02	3.06	3.08	3.16
CoOp + CMP ($\lambda_1 = 0$)	3.18	3.42	3.32	3.12	2.88	3.48	3.50	3.32	3.08	3.12	3.12	3.24
ECE												
$\Delta \%$	3.25 \uparrow	2.09 \uparrow	2.47 \uparrow	1.96 \uparrow	2.70 \downarrow	3.57 \uparrow	3.55 \uparrow	2.47 \uparrow	1.99 \uparrow	1.96 \uparrow	1.30 \uparrow	2.53 \uparrow
CoOp	3.08	3.35	3.24	3.06	2.96	3.36	3.38	3.24	3.02	3.06	3.08	3.16
CoOp + FIM ($\lambda_2 = 0$)	3.05	3.30	3.20	3.00	2.84	3.30	3.32	3.18	2.96	3.00	3.02	3.10
$\Delta \%$	0.97 \downarrow	1.49 \downarrow	1.23 \downarrow	1.96 \downarrow	4.05 \downarrow	1.79 \downarrow	1.78 \downarrow	1.85 \downarrow	1.99 \downarrow	1.96 \downarrow	1.94 \downarrow	1.90 \downarrow

Table 6. Accuracy three datasets for tuning λ_1 within range (0.0 – 1.0) while keeping λ_2 value fixed 0.

Datasets				
λ_1	Flowers102	Food101	UCF101	DTD
0.0	83.5	96.2	83.5	53.1
0.2	81.3	94.8	83.1	53.5
0.4	85.5	98.7	84.3	55.1
0.6	84.7	90.8	80.4	52.2
0.8	82.4	89.1	82.9	52.2
1.0	81.8	87.0	80.9	51.5

Table 7. Expected Calibration Error (ECE) for tuning λ_2 in range (0.0 – 1.0) with $\lambda_1 = 0$.

Datasets				
λ_2	Flowers102	Food101	UCF101	DTD
0.0	6.27	5.69	5.21	4.13
0.2	4.61	4.36	4.04	3.66
0.4	3.16	3.02	2.94	2.92
0.6	3.56	3.54	3.24	3.15
0.8	4.26	4.18	3.74	3.39
1.0	5.22	5.17	4.48	3.89